Dose-Dependent Pharmacokinetics of the Aldose Reductase Inhibitor Imirestat in Man

R. Kim Brazzell,[1,4] Philip R. Mayer,[1] Richard Dobbs,[1] Patrick J. McNamara,[2] Renli Teng,[2] and John T. Slattery[3]

Received January 9, 1990; accepted July 11, 1990

The pharmacokinetics of imirestat were studied in healthy volunteers following single and multiple oral doses. After single doses of 20 to 50 mg, imirestat plasma concentrations declined with an apparent elimination half-life of 50 to 70 hr over the 168 hr in which levels were measured. However, with lower doses (2 to 10 mg), an initial rapid decline in drug concentration was followed by a very slow terminal elimination phase with plasma concentrations decreasing little over the 1 week of sampling. This resulted in a decrease in apparent $t_{1/2}$ with increasing dose, from 272 ± 138 hr at 2 mg to 66 ± 30 hr at 50 mg. During once-daily dosing of 2 to 20 mg/day for 4 weeks, mean steady-state imirestat concentrations appeared to be dose proportional, although the time required to achieve steady state decreased with increasing dose. The mean effective half-life for accumulation ranged from 54 to 98 hr, suggesting that the very slow elimination of drug at low concentrations did not produce disproportionate accumulation of drug at these doses. Mean oral clearance was independent of dose, ranging from 30 to 45 ml/min. At the 2-, 5-, and 20-mg doses, one subject in each group had steady-state concentrations two- to fourfold greater than any of the other five subjects at the same dose, although the reason for this was not apparent from these data. The overall kinetic profile of these data was suggestive of dose-dependent pharmacokinetics resulting from nonlinear tissue binding of imirestat. A two-compartment pharmacokinetic model incorporating saturable binding in the tissue compartment and elimination from the central compartment was developed and provided a good description of the plasma concentration data after both single and multiple dosing.

KEY WORDS: aldose reductase inhibitors; imirestat; dose-dependent pharmacokinetics; tissue binding.

INTRODUCTION

Recent studies have indicated that excessive metabolic conversion of glucose to sorbitol by the aldose reductase enzyme may contribute to the complications associated with diabetes mellitus (1–3), particularly the development of neuropathy (4), cataract (5), and retinopathy (6). As a result of this evidence, aldose reductase inhibitors are being evaluated for their potential to prevent some of the pathological consequences of diabetes (7,8). Imirestat [2,7-difluoro-spiro-(9H-fluorene-9,4′-imidazolidine)-2′,5′-dione; AL01576; HOE843] is a potent aldose reductase inhibitor that has been shown to prevent sorbitol accumulation in the peripheral nerves and lens of diabetic animals and to prevent the development of altered nerve function and cataracts (5,9,10). This report describes the pharmacokinetics of imirestat in healthy volunteers following single and multiple oral doses.

Imirestat is a weak acid with a pK_a of 7.35 and low aqueous solubility. The drug is approximately 85% bound to plasma protein, with binding being highly pH dependent in the range of physiologic pH (11). The pharmacokinetics of imirestat in several species are characterized by low clearance, intermediate volume of distribution and a long biologic half-life (12). Following single iv and oral dosing to rats, ^{14}C-imirestat persists in certain tissues, such as the eye, testes, adrenals, and kidney, with the tissue-to-plasma concentration ratio increasing substantially over a 1-week period following a single dose (13). Following topical ocular dosing to rabbits, imirestat is retained by the cornea and lens and is slowly eliminated from both tissues with a half-life of approximately 140 hr (14). Many of the tissues by which imirestat is preferentially retained (i.e., lens, kidney, testes, adrenals) are known to contain significant amounts of the aldose reductase enzyme (15–18). This, along with the high affinity of the drug for aldose reductase (10), has led to speculation that binding of imirestat to the aldose reductase enzyme may play a role in the very slow elimination of drug from both the eye and the body (13,14). The purpose of this study was to determine if imirestat exhibits pharmacokinetic characteristics in humans compatible with the tissue persistence observed in animals.

METHODS

Single-Dose Study

Thirty-six healthy male volunteers ranging in age from 21 to 59 years (mean, 32 ± 9 years) and in weight from 55 to 98 kg (mean, 73 ± 11 kg) participated in the study. Each was judged to be in good health based upon physical examination, medical history, clinical laboratory tests, vital signs, and EKG. The subjects were confined to the clinical research unit (Quincy Laboratories, Kansas City, MO) for 12 hr prior to drug treatment and for 7 days thereafter.

Single oral doses of 2, 10, 20, 30, 40, and 50 mg of imirestat were given to separate groups of six subjects each at approximately 8 AM following an overnight fast. Blood specimens were collected prior to dosing and at 1, 2, 4, 6, 8, 12, 24, 36, 48, 60, 72, 96, 120, 144, and 168 hr after dosing for analysis of drug concentration. Urine specimens (total volume voided) were collected at the following intervals after dosing: 0–4, 4–8, 8–12, 12–24, 24–48, 48–72, 72–96, 96–120, 120–144, and 144–168 hr.

Multiple-Dose Study

Once-daily oral doses of 2, 5, 10, and 20 mg of imirestat were administered to four groups of six healthy male volunteers each for 28 days. These subjects ranged in age from 23 to 58 years (mean, 39 ± 10 years) and in weight from 56 to 93

[1] Research and Development, Alcon Laboratories, Inc., 6201 South Freeway, Fort Worth, Texas 76134.

[2] Division of Pharmacology and Experimental Therapeutics, College of Pharmacy, University of Kentucky, Lexington, Kentucky 40536.

[3] Department of Pharmaceutics, University of Washington, Seattle, Washington 98195.

[4] To whom correspondence should be addressed.

kg (mean, 73 kg ± 8 kg) and were judged to be of good health as above. The subjects were confined to the clinical research unit (Quincy Laboratories, Kansas City, MO) for 12 hr before the first dose, during the entire 28 days of dosing and for 7 days thereafter. Subjects fasted for approximately 8 hr prior to each morning dose. Plasma specimens were collected prior to and 1, 2, 4, 8, 12, and 24 hr after the first dose and immediately before dosing on Days 3, 4, 5, 6, 7, 9, 11, 14, 17, 20, 24, and 28. After the last dose on Day 28, plasma samples were collected at 1, 2, 4, 8, 12, 24, 36, 48, 60, 72, 96, 120, 144, and 168 hr. Two subjects in the 10-mg dose group withdrew from the study prior to completion for reasons unrelated to the test medication. Therefore complete data were collected for only four subjects at 10 mg.

Analytical Methods

Plasma imirestat concentrations from the 10- through the 50-mg single oral doses and urine concentrations following all single doses were determined by a reverse phase HPLC method. The method involved extraction of the plasma specimens with C_{18} solid phase columns and chromatography of the sample utilizing a Spherisorb ODS 5-μm column with a mobile phase of acetonitrile:0.5% phosphate buffer, pH 7.2 (300:700, v/v). The assay was linear over the range of 10 to 5000 ng/ml (r^2 = 0.998), with the interassay coefficient of variation ranging from 1.5% at 5000 ng/ml to 11% at 10 ng/ml.

Plasma imirestat concentrations from the 2-mg single dose and all of the multiple doses were measured by a gas chromatographic electron capture assay method. This method has been described elsewhere (19,20) and involves cleanup of 0.5 ml or smaller plasma specimens in a similar fashion to that for the HPLC assay followed by derivatization with pentafluorobenzyl bromide. After purification of the derivative, the extract was analyzed using a Hewlett-Packard Model 5809A gas chromatograph equipped with a 30-m fused silica (0.25-mm-ID) SPB-1 column and ^{63}Ni ECD. The assay was linear over the range of 2.5 to 200 ng/ml (r^2 = 0.999), with the interassay coefficient of variation ranging from 4% at 200 ng/ml to 11% at 25 ng/ml. For samples with concentrations higher than 200 ng/ml, smaller plasma aliquots were diluted to provide concentrations within the validated range. Comparison of the HPLC and GC assays demonstrated that the two methods gave equivalent results over the validated range of concentrations.

Pharmacokinetics

Estimates of the terminal elimination rate constant (β) were obtained by linear regression analysis of the terminal log-linear portion of the plasma concentration-time curve; the corresponding half-life ($t_{1/2}$) was calculated by dividing 0.693 by β. The area under the plasma concentration–time curve from 0 to 24 hr (AUC_{24}) after both the first and the last dose of the multiple dosing regimens was calculated for each subject by linear trapezoidal summation. The accumulation of drug during multiple dosing was characterized by the accumulation ratio, R:

$$R = \frac{AUC_{24}\ (\text{last dose})}{AUC_{24}\ (\text{first dose})}$$

From R, the effective half-life for accumulation ($t_{1/2}$ acc) was calculated via the following equation (21):

$$t_{1/2}\ \text{acc} = \frac{\ln 2 \times \tau}{\ln [R/(R-1)]}$$

where τ is the dosing interval (24 hr). Apparent oral clearance (CL_{po}) was calculated as dose divided by AUC_{24} of the last dose assuming the fraction of the dose absorbed to be 1.

The plasma concentration–time data from the single dose study were fitted with a two-compartment model incorporating saturable tissue binding in the peripheral compartment. This model is depicted in Fig. 1 and equations of the model are developed in the Appendix. The model consists of two physiological spaces (vascular and nonvascular) interconnected by a diffusional clearance term (CL_{du}) with elimination from the vascular (central) pool (CL_u). Drug absorption was assumed to be rapid and complete. Both clearance terms (CL_{du} and CL_u) were a function of unbound drug and binding in both compartments was described by a Langmuir-type isotherm. Binding was linear in the vascular space (central compartment) with a constant free fraction of 0.14, relating to 86% binding to plasma proteins (11). Binding in the nonvascular (tissue) compartment was nonlinear. In order to facilitate the fitting procedure, the following parameters of the model were fixed as constants.

V_1: Central or vascular space volume (3.15 liters)
V_2: Peripheral or nonvascular space volume (41.8 liters)
f_u: Fraction unbound in vascular compartment (0.14).

The fitted parameters were as follows.

CL_{du}: Intercompartmental diffusion clearance of unbound drug (liters/hr)
CL_u: Systemic clearance of unbound drug (liters/hr)
NP_2: Tissue binding capacity constant (μg/ml)
KA_2: Tissue binding affinity constant (ml/μg)

Initial estimates were obtained via various methods. An average plasma free fraction of 0.14 was used which was consistent with previous *in vitro* protein binding results (11). The mean data for the low dose was fitted with a biexponential function to estimate slopes and intercepts for the "linear" case assumption. The resulting parameters were used to estimate micro-rate constants for a two compartment model (i.e., k_{10}, k_{12}, k_{21}).

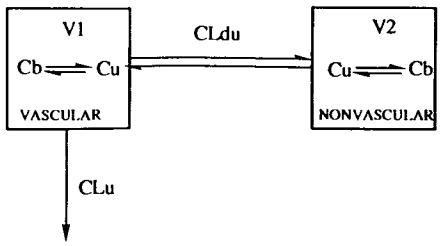

Fig. 1. Pharmacokinetic model used to analyze the imirestat plasma concentration-time data. Binding in the vascular compartment is linear and binding in the nonvascular tissue compartment is nonlinear.

Clearance parameters (CL_u and CL_{du}) were then estimated from the following relationships:

$$CL_{du} = k_{12}V_1/f_u, \qquad CL_u = k_{10}V_1/f_u$$

Initial estimates for the tissue binding parameters (NP_2 and KA_2) were obtained via trial and error using simulations. Final estimates of the parameters (CL_{du}, CL_u, NP_2, KA_2) were obtained by simultaneous fitting of the mean data from the six single doses to the equations describing the model using NONLIN (22). In addition, six sets of individual concentration–time profiles (one subject from each dose) were also simultaneously fitted with these model equations to confirm the validity of using mean data and to get an appreciation of intersubject variability.

RESULTS

The imirestat plasma concentration–time curves from the individual subjects following single doses of 2, 10, and 50 mg are shown in Fig. 2. These data illustrate the dose-dependent pharmacokinetics of imirestat, with very slow elimination of drug from plasma at low doses (2 and 10 mg) and considerably faster elimination at the higher dose. The lower doses are characterized by an initial rapid decrease in plasma concentration followed by a very slow decline from 12 to 168 hr. Accurate $t_{1/2}$ could not be calculated from these data because of the very slow elimination but could be estimated by the linear regression analysis. At the 2-mg dose, apparent $t_{1/2}$ ranged from 109 to 430 hr ($\bar{X}$ = 272 ± 138 hr) and at 10 mg from 46 to 417 hr ($\bar{X}$ = 114 ± 143 hr). At the 50-mg dose, plasma concentrations declined substantially faster over the 168-hr observation period than after either of the lower doses, with apparent $t_{1/2}$ ranging from 38 to 125 hr ($\bar{X}$ = 66 ± 30 hr). Very little intact imirestat (<1% of dose) was detected in the urine, with no drug detectable in many of the specimens. Thus pharmacokinetic analysis of the urinary excretion data was not possible.

The observed kinetic behavior was incompatible with linear pharmacokinetic models, and therefore the data were fit to the nonlinear tissue binding model shown in Fig. 1. Figure 3 shows the fit of this pharmacokinetic model to the mean single-dose data at the six doses studied. Overall visual agreement between the actual and the fitted curves was good, although there are some systematic deviations at the lower doses. Parameter values are shown in Table I. There was good agreement between the parameter estimates from the mean data and the randomly grouped individual data (Table 1), providing some assurance that the kinetic phenomenon observed for the mean data is reflective of the individual profiles. The values derived from the grouped individual data sets also provides some insight into the intersubject variability of the model parameters.

The mean trough plasma concentration data over the 28 days of dosing at the 2-, 5-, 10-, and 20-mg daily doses are presented in Fig. 4, along with computer-simulated curves from the nonlinear tissue binding model using parameter estimates from the single-dose fits (Table 1). Accumulation of drug during multiple dosing resulted in steady-state concen-

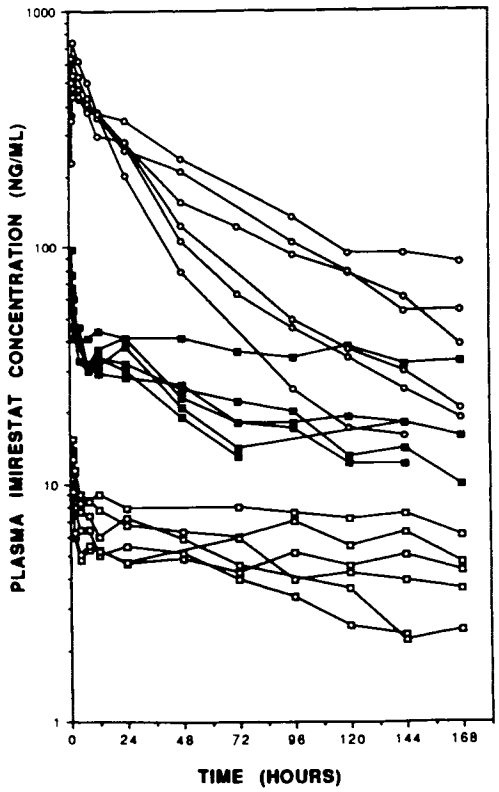

Fig. 2. Individual imirestat plasma concentration-time profiles after the 2-mg (□), 10-mg (■), and 50-mg (○) single doses.

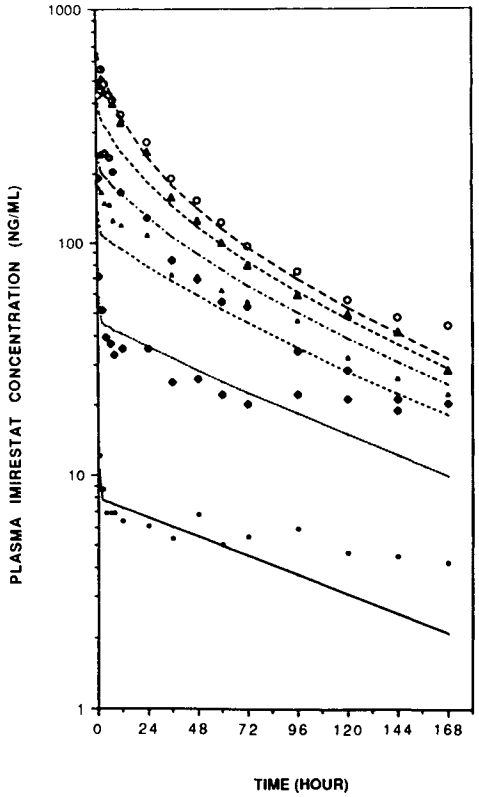

Fig. 3. Mean imirestat plasma concentration–time data from the 2-mg (●), 10-mg (♦), 20-mg (△), 30-mg (◇), 40-mg (▲), and 50-mg (○) single doses along with the best fits of the data to the nonlinear tissue binding pharmacokinetic model.

Table I. Parameter Estimates from Simultaneously Fitting Mean Imirestat Plasma Concentration Data from the 2-, 10-, 20-, 30-, 40-, and 50-mg Single Doses to the Nonlinear Tissue Binding Model and from Fits of Randomly Grouped Individual Sets of Data

	CL_{du} (L/hr)	CL_u (L/hr)	NP_2 (μg/ml)	KA_2 (ml/μg)
Mean data	109 (13)[a]	12.6 (0.42)	1253 (103)	0.027 (0.003)
Randomly grouped individual data				
Set 1	111	17.2	1046	0.032
Set 2	98	11.9	1388	0.022
Set 3	106	16.3	941	0.038
Set 4	102	14.8	919	0.044
Set 5	101	14.6	1217	0.028
Set 6	102	16.7	1366	0.021
Mean	103	15.3	1146	0.031
(SD)	(4.7)	(2.0)	(208)	(0.009)

[a] Standard deviation estimates from NONLIN are shown in parentheses.

trations approximately four to six times those seen with single doses, with apparent steady state being achieved within 2 weeks in most subjects. At the 2-, 5-, and 20-mg doses, one subject in each group (Nos. 78, 184, and 93) accumulated considerably more drug than any of the other five subjects and were therefore excluded from the mean data in Fig. 4. The tissue binding model describes the observed data quite well. Of particular interest is that the time to reach steady state decreases with increasing dose in both the observed data and the computer simulations.

Individual plasma concentration–time profiles following the last dose of multiple dosing at 2, 5, and 20 mg/day are shown in Fig. 5. These data viewed collectively further demonstrate the nonlinear pharmacokinetics of imirestat, with the shapes of the plasma concentration–time profiles being dependant on the dose given and the magnitude of the resulting plasma concentrations. These data also show the three outlying subjects discussed above, with approximately twofold higher concentrations than the other subjects at the 2- and 5-mg doses and fivefold higher at the 20-mg dose.

Model-independent parameters calculated from the multiple-dose data are presented in Table II. With the exception of the outlying subjects (78, 184 and 93), CL was fairly consistent among individuals, ranging from 30 to 50 ml/min, and appeared to be independent of dose. CL of the three outlying subjects were considerably less than the other subjects, ranging from 10 to 16 mL/min. AUC_{24} after the first dose for these three subjects were no different from those for the other subjects in their respective groups, but AUC_{24} after the last dose was two- to threefold higher. The accumulation ratio, R, ranged from 3 to 7 for all subjects but these three, whose values were 11–12. Without these outlying values, mean R was quite similar at the 2-, 5-, and 10-mg doses (5.3–5.6) and somewhat less at 20 mg (3.7). Calculation of $t_{1/2}$ from the actual plasma concentration data after the last dose was not possible because of the shapes of the washout

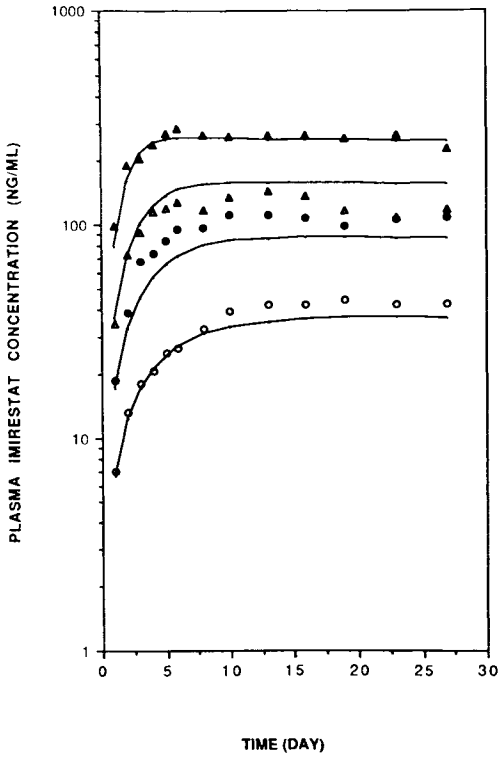

Fig. 4. Mean imirestat plasma concentrations during the 28 days of multiple dosing at 2 (○), 5 (●), 10 (△), and 20 (▲) mg/day with simulations generated with the nonlinear tissue binding model using the parameter estimates from the single-dose fits. (Data from subjects 78, 184, and 93 have been excluded from the means; see text.)

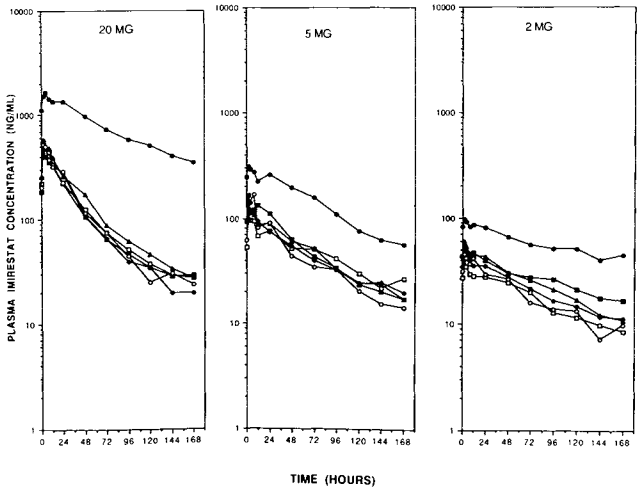

Fig. 5. Individual imirestat plasma concentration–time profiles following the last dose of multiple dosing at 2, 5, and 20 mg/day.

Table II. Pharmacokinetic Parameters from Individual Subjects During Multiple Dosing of Imirestat to Healthy Volunteers

Dose (mg)	Subject	AUC_{24} ($\mu g \cdot hr \cdot ml^{-1}$) First dose	AUC_{24} ($\mu g \cdot hr \cdot ml^{-1}$) Last dose	R^a	$t_{1/2}$ acc (hr)[b]	CL_{po} (ml/min)
2	71	0.15	1.06	7.04	108	31
	73	0.18	0.92	5.11	76	36
	74	0.16	0.73	4.54	67	45
	75	0.21	1.12	5.40	81	30
	77	0.21	0.90	4.38	64	37
	78	0.17	2.06	12.08	192	16
	$\bar{X} \pm SD$[c]	0.18 ± 0.02	1.13 ± 0.47	6.42 ± 2.92	98 ± 49	33 ± 10
	$\bar{X} \pm SD$[d]	0.18 ± 0.03	0.95 ± 0.15	5.29 ± 1.06	79 ± 18	36 ± 6
5	183	0.54	3.01	5.54	84	28
	184	0.57	6.21	10.94	174	13
	185	0.36	1.94	5.35	80	43
	187	0.42	2.45	5.78	88	34
	188	0.47	2.56	5.47	82	33
	189	0.44	2.35	5.38	81	36
	$\bar{X} \pm SD$[c]	0.47 ± 0.08	3.09 ± 1.57	6.41 ± 2.72	98 ± 37	31 ± 10
	$\bar{X} \pm SD$[e]	0.45 ± 0.07	2.46 ± 0.39	5.50 ± 0.17	83 ± 3	35 ± 6
10	80	0.77	3.21	4.20	61	52
	81	0.67	4.72	7.09	109	35
	82	0.59	3.42	5.80	88	49
	85	0.72	3.77	5.21	78	44
	$\bar{X} \pm SD$[c]	0.69 ± 0.08	3.77 ± 0.67	5.57 ± 1.21	84 ± 20	45 ± 7
20	87	1.81	7.90	4.37	64	42
	88	2.44	9.47	3.89	60	35
	89	2.35	8.84	3.76	54	38
	90	3.11	9.83	3.16	44	34
	92	2.63	8.69	3.31	46	38
	93	2.94	33.88	11.5	183	9.9
	$\bar{X} \pm SD$[c]	2.54 ± 0.46	13.1 ± 10.2	5.00 ± 3.21	75 ± 53	33 ± 12
	$\bar{X} \pm SD$[f]	2.45 ± 0.47	8.95 ± 0.75	3.69 ± 0.48	54 ± 9	38 ± 3

[a] R = [AUC_{24} (last dose)/AUC_{24} (first dose)].
[b] Calculated from R.
[c] Mean calculated using data from all subjects.
[d] Mean calculated without data from subject 78.
[e] Mean calculated without data from subject 184.
[f] Mean calculated without data from subject 93.

curves, which changed continuously over the 168-hr washout period due to the slow transition into the terminal elimination phase. Therefore, an effective half-life for accumulation ($t_{1/2}$ acc) was calculated from the accumulation parameters from the first and last doses of the multidose data. The accumulation half-life was similar between subjects (excluding Nos. 78, 184, and 93), with mean values of 79, 83, and 84 hr at the 2-, 5-, and 10-mg doses and somewhat less (54 hr) at the 20-mg dose.

DISCUSSION

The data presented in this report illustrate a complex and intriguing pharmacokinetic profile for imirestat, characterized by apparent saturable tissue binding that results in a slow terminal elimination phase. These data also demonstrate that the pharmacokinetics of imirestat in humans are consistent with the persistence of the drug in tissues observed previously in rats (13). In the model-independent analysis, apparent oral clearance was independent of dose (Table II) and apparent half-life decreased with increasing dose. The overall nature of the kinetic profile observed here, particularly the dose dependency of drug elimination half-life but not clearance, is suggestive of saturable tissue binding of imirestat (23). The ability of the nonlinear tissue binding pharmacokinetic model to describe adequately the observed pharmacokinetic data following both single and multiple doses supports this hypothesis.

The data from the multiple-dose studies indicate that the observed persistence at low plasma concentrations was not associated with disproportionate accumulation of drug during multiple dosing at these doses, although it did appear to influence accumulation rate (i.e., the time to reach steady state). Steady-state concentrations were proportional to

dose and the time to steady state decreased with increasing dose (Fig. 4), in accord with the properties of the nonlinear tissue binding model as described previously (24). A saturable terminal elimination phase would not be expected to effect accumulation rate in the same manner as with linear pharmacokinetics. Instead, a one-time contribution of this phase to accumulation would be expected, such that once the tissue pools are saturated, accumulation rate would be governed by the effective elimination half-life, which appears to be 50 to 70 hr, and would be proportional to dose.

Three of the subjects in the multiple-dose study (one each at the 2-, 5-, and 20-mg doses) achieved greater than twofold higher steady-state plasma concentrations than the other five subjects in each respective group, despite achieving similar concentrations after the first dose. The reason for this phenomenon is unknown, but somewhat slower elimination in two of these subjects (Fig. 5) suggests that genetic polymorphic drug metabolism may be involved in the elimination of the drug. Preliminary data indicate that aromatic hydroxylation is a pathway for biotransformation of imirestat, and genetic differences in the rate of metabolism have been demonstrated for several drugs undergoing this type of metabolic conversion.

Saturable tissue binding of drugs has been observed previously, although the therapeutic relevance of this phenomenon seems to differ from drug to drug. Methotrexate is very tightly bound to the target enzyme, dihydrofolate reductase, resulting in very slow decline of plasma concentrations of the drug at concentrations below 10^{-7} *M* (25,26). However, antifolate activity is believed to require a completely saturated enzyme and freely exchangeable unbound drug in the cytosol (27). Therefore, although drug persists at low plasma levels, effect is not associated with this persistence, since concentrations higher than 10^{-7} *M* are needed to completely saturate dihydrofolate reductase and block the conversion of dihydrofolate to tetrahydrofolate.

On the other hand, the antiulcer drug omeprazole has a relatively short plasma half-life but persists at the site of action for an extremely long period, due to binding to the specific ATPase involved in the proton pump in the GI tract (28,29). In this case, the pharmacologic effect is associated with the persistent tissue levels of drug and the observed plasma concentration–time profile is not predictive of the time course of effect.

It is not known whether the persistence of imirestat in tissue is due to nonspecific tissue binding or binding to the target enzyme, aldose reductase. The latter seems possible since tissues in which the drug persists in rats (i.e., kidney, testes, adrenals, eye) are known to have a high concentration of aldose reductase (15–18). However, even if the drug dissociates very slowly from the target enzyme, it is not clear whether the pharmacologic effect would persist (as with omeprazole) or be lost (as with methotrexate).

Both imirestat and omeprazole are new drugs specifically selected for their very high affinity for their target enzymes. The pharmacokinetic characteristics of other drugs have also been shown to be related to their high affinity for the target enzyme (e.g., various ACE inhibitors, which display saturable binding to plasma ACE). We expect that the phenomenon described here for imirestat will be observed with increasing frequency, as more potent and specific enzyme inhibitors are designed. The therapeutic significance of persistent low plasma drug concentrations is likely to vary from enzyme to enzyme and drug to drug.

In conclusion, it appears that imirestat has a complex pharmacokinetic profile characterized by prolonged persistence of drug at low concentrations. This persistence of drug is likely the result of high-affinity binding to tissue, perhaps the aldose reductase enzyme, but does not appear to have significant impact upon accumulation of drug during multiple dosing at doses of 2 to 20 mg. A two-compartment pharmacokinetic model incorporating saturable binding of imirestat in tissue provided a good description of the observed plasma concentration data and should be useful for providing further understanding of the pharmacokinetics of this compound.

APPENDIX

For the model shown in Fig. 1, the rates of change of the drug in physiological (vascular and nonvascular) spaces following an intravenous bolus injection can be described as

$$V_1 \frac{dC_1^t}{dt} = CL_{du}\,(C_2^u - C_1^u) - CL_u\,C_1^u \qquad (A1)$$

and

$$V_2 \frac{dC_2^t}{dt} = CL_{du}\,(C_1^u - C_2^u) \qquad (A2)$$

where (and thereafter) the superscript t, u, and b denote, respectively, the total, unbound, and bound drug, the subscript 1 and 2 refer to the central (vascular) and peripheral (nonvascular) space, V is the volume of the space, C is the concentration of drug, CL_{du} is the diffusion clearance between the two spaces, and CL_u is the unbound systemic clearance from vascular space. The total concentration of drug at any time in the nonvascular spaces can be expressed as

$$C_2^t = C_2^u + C_2^b \qquad (A3)$$

Assuming that the concentration of drug bound to the protein can be described by a Langmuir-type isotherm consistent with a single class of noninteraction binding sites, then

$$C_2^t = C_2^u\left[1 + \frac{NP_2KA_2}{1 + KA_2\,C_2^u}\right] \qquad (A4)$$

where NP is the concentration of binding sites (or capacity constant) and KA is the binding affinity constant. The differentiation of Eq. (A4) with respect to time yields

$$\frac{dC_2^t}{dt} = \frac{dC_2^u}{dt}\left[1 + \frac{NP_2KA_2}{1 + KA_2C_2^u} - \frac{NP_2KA_2^2\,C_2^u}{(1 + KA_2\,C_2^u)^2}\right] \qquad (A5)$$

Substitution of Eq. (A5) in Eq. (A2) yields

$$V_2 \frac{dC_2^u}{dt}\left[1 + \frac{NP_2\,KA_2}{1 + KA_2\,C_2^u} - \frac{NP_2\,KA_2^2\,C_2^u}{(1 + KA_2\,C_2^u)^2}\right] = CL_{du}(C_1^u - C_2^u) \qquad (A6)$$

Rearrangement yields

$$V_2 \frac{dC_2^u}{dt} = \frac{CL_{du}(C_1^u - C_2^u)}{1 + [NP_2\ KA_2/(1 + KA_2C_2^u)^2]} \quad (A7)$$

Because the unbound fraction of drug in vascular space (f_u) is constant, the substitution of $C_1^t f_u$ for C_1^u in Eqs. (A1) and (A7) yields

$$V_1 \frac{dC_1^t}{dt} = CL_{du}(C_2^u - C_1^t f_u) - CL_u\ C_1^t f_u \quad (A8)$$

$$V_2 \frac{dC_2^u}{dt} = \frac{CL_{du}\ (C_1^t f_u - C_2^u)}{1 + [NP_2\ KA_2/(1 + KA_2C_2^u)^2]} \quad (A9)$$

The differential Eqs. (A8) and (A9) were fitted, simultaneously, with the observed data to obtain estimates of KA_2, NP_2, CL_u, and CL_{du}. These equations were also used to generate values of C_1^t and C_2^u as a function of time for single and multiple doses.

REFERENCES

1. K. H. Gabbay. The sorbitol pathway and the complications of diabetes. *N. Engl. J. Med.* 288:831–836 (1973).
2. J. H. Kinoshita, S. Fukushi, P. Kador, and L. O. Merola. Aldose reductase in diabetic complications of the eye. *Metabolism* 28 (Suppl. 1):462–469 (1979).
3. K. H. Gabbay, L. O. Merola, and P. A. Field. Sorbitol pathway: Presence in nerve and cord with substrate accumulation in diabetes. *Science* 151:209–210 (1966).
4. R. S. Clements. Diabetic neuropathy-new concepts of its etiology. *Diabetes* 28:604–611 (1979).
5. M. L. Chandler, J. Boltralik, B. York, and L. DeSantis. Prevention of cataracts in diabetic rats by aldose reductase inhibitors. *Invest. Ophth. Vis. Sci.* 22:156 (1982).
6. W. G. Robinson, P. F. Kador, and J. H. Kinoshita. Retinal capillaries: Basement membrane thickening by galactosemia prevented with aldose reductase inhibitor. *Science* 221:1177–1179 (1983).
7. D. J. Handelsman and J. R. Turtle. Clinical trials of an aldose reductase inhibitor in diabetic neuropathy. *Diabetes* 30:459–464 (1981).
8. R. J. Young, D. J. Ewing, and B. F. J. Clarke. A controlled trial of sorbinil, an aldose reductase inhibitor, in chronic painful diabetic neuropathy. *Diabetes* 32:938–942 (1983).
9. M. L. Chandler, W. A. Shannon, and L. DeSantis. Prevention of retinal capillary basement membrane thickening in diabetic rats by aldose reductase inhibitors. *Invest. Ophthalmol. Vis. Sci.* 25 (Suppl.):159 (1984).
10. B. W. Griffin, L. G. McNatt, M. L. Chandler, and B. M. York. Effects of two new aldose reductase inhibitors, AL01567 and AL01576, in diabetic rats. *Metabolism* 36:486–490 (1987).
11. P. J. McNamara, R. A. Blouin, and R. K. Brazzell. Serum protein binding of AL01576, a new aldose reductase inhibitor. *Pharm. Res.* 5:319–321 (1988).
12. R. K. Brazzell, Y. H. Park, C. B. Wooldridge, B. McCue, R. Barker, and B. York. Interspecies comparison of the pharmacokinetics of aldose reductase inhibitors. *Drug Metab. Disp.* 18: 435–440 (1990).
13. Y. H. Park, C. B. Wooldridge, J. Mattern, M. L. Stoltz, and R. K. Brazzell. Disposition of the aldose reductase inhibitor AL01576 in rats. *J. Pharm. Sci.* 77:110–115 (1988).
14. R. K. Brazzell, C. B. Wooldridge, R. B. Hackett, and B. A. McCue. Pharmacokinetics of the aldose reductase inhibitor imirestat following topical ocular administration. *Pharm. Res.* 7:192–198 (1990).
15. C. M. Sheaff and C. C. Doughty. Physical and kinetic properties of homogenous bovine lens aldose reductase. *J. Biol. Chem.* 251:2696–2702 (1976).
16. K. H. Gabbay and E. S. Cathcart. Purification and immunologic identification of aldose reductose. *Diabetes* 23:460–468 (1974).
17. M. A. Ludvigson and R. L. Sorenson. Immunohistochemical localization of aldose reductase. *Diabetes* 29:438–459 (1980).
18. C. E. Grimshaw and E. J. Mathur. Immunoquantitation of aldose reductase in human tissues. *Anal. Biochem.* 176:66–71 (1989).
19. B. McCue, Y. H. Park, and R. K. Brazzell. Capillary gas chromatographic (GCEC) assay for the aldose reductase inhibitor AL01576 (HOE843), in lens and plasma. *Pharm. Res.* 5:S29 (1988).
20. O. Hockwin, P. Müller, J. Krolczyk, B. A. McCue, and P. R. Mayer. Determination of AL01576 concentration in rat lenses and plasma by bioassay for aldose reductase activity measurements. *Ophth. Res.* 21:285–291 (1989).
21. G. Kaiser, R. Ackermann, S. Brechbühler, and W. Dieterle. Pharmacokinetics of the angiotensin converting enzyme inhibitor benazepril:HCl (CGS 14824A) in healthy volunteers after single and repeated administration. *Biopharm. Drug. Dispos.* 10:365–376 (1989).
22. C. M. Metzler, G. L. Elfring, and A. J. McEwen. Package of computer programs for pharmacokinetic modeling. *Biometrics* 30:562–563 (1974).
23. M. Gibaldi, G. Levy, and P. J. McNamara. Effect of plasma protein and tissue binding on biologic half-life of drugs. *Clin. Pharm. Ther.* 24:1–4 (1978).
24. P. J. McNamara, J. T. Slattery, M. Gibaldi, and G. Levy. Accumulation kinetics of drugs with nonlinear protein and tissue binding characteristics. *J. Pharmacokin. Biopharm.* 7:397–405 (1979).
25. C. L. Zimmerman, T. J. Franz, and J. T. Slattery. Persistence of antifolate activity in skin of rats following systemic administration of methotrexate. *J. Invest. Derm.* 82:57–61 (1983).
26. C. L. Zimmerman, T. J. Franz, and J. T. Slattery. Time course of methotrexate and its polyglutamates in tissues of rat and hairless mouse. *J. Pharmacol Exp. Ther.* 231:242–247 (1984).
27. J. C. White and I. D. Goldman. Mechanisms of action of methotrexate: IV. Free intracellular methotrexate required to suppress dihydrofolate reduction to tetrahydrofolate by Erlich ascites tumor cells *in vitro*. *Mol. Pharmacol* 12:711–719 (1976).
28. H. F. Helander, C. H. Ramsay, and C. G. Regardh. Localization of omeprazole and metabolites in the mouse. *Scand. J. Gastroent.* 20(S108):95–104 (1985).
29. C. Cederberg, G. Ekenved, T. Lind, and L. Olbe. Acid inhibitory characteristics of omeprazole in man. *Scand. J. Gastroent.* 20(S108):105–112 (1985).